Validation of a novel discrete-based model for fracturing of brittle materials

Somayeh Behraftar[a,b,*], Sergio Galindo Torres[a,b], Alexander Scheuermann[a,b], David J. Williams[b], Eduardoantonio G. Marques[c], Hossein Janjani[d]

[a]Research Group on Complex Processes in Geo-Systems, The University of Queensland, Brisbane QLD 4072, Australia
[b]Geotechnical Engineering Centre, School of Civil Engineering, The University of Queensland, Brisbane QLD 4072, Australia
[c]Departament of Civil Engineering, Federal University of Viosa, Campus Universitrio, Viosa (MG), 36570-000, Brazil
[d]Geotechnical Engineer, Douglas Partners Pty Ltd, Brisbane, Australia

Abstract

In this study, a micro-mechanical model is developed to study the fracture propagation process in rocks. The model is represented by an array of bonded particles simulated by the Discrete Sphero-Polyhedra Element Model (DSEM), which was introduced by the authors previously. It allows the modelling of particles of general shape, with no internal porosity. The DSEM method is used to model the Crack Chevron Notch Brazilian Disc (CCNBD) test suggested by the International Society of Rock Mechanics (ISRM) for determining the fracture toughness of rock specimens. CCNBD specimens with different crack inclination angles relative to the direction of loading are modelled to investigate the fracture geometry and propagation. The Crack Mouth Opening Displacement (CMOD) is calculated, and the results are validated using experimental results obtained from the literature. The motivation behind using this technique is the desire to study micro-mechanical aspects of fracture propagation in rocks and to formulate calibration procedures for the quantitative modelling of rock materials using discrete approaches. The results from this study contribute to the proper validation of discrete methods and improved understanding of how micro-damage affects fracture at the macro scale.

Keywords: Brittle Rock, Crack Mouth Opening Displacement, Cracked Chevron Notched Brazilian Disc, Discrete Element Method

1. Introduction

Predicting the failure load in brittle materials such as rocks that contain pre-existing cracks, and determining the effect of the load and crack geometry on failure, are important in the design of structures in such materials. In order to study the failure process, the prediction of the trajectory of crack propagation in the brittle material is an important question that needs to be addressed. Depending on the direction of the applied load, a crack propagates through by one of three different modes (mode I, II and III) or mixed modes [1]. Mode I is the tensile opening mode, resulting in normal stresses applied at the crack tip and lead to the opening the crack. Mode II is the in-plane sliding or shearing mode, acting in the direction of crack extension. Mode III is tearing, or the anti-plane mode, in which the crack surfaces shear relative to each other [1] (Fig. 1). Pre-existing cracks and discontinuities in rocks are not only subjected to direct tensile loading, but also to compressive, shear or mixed modes of loading. The tensile mechanism of rock fracture may not be sufficient to explain rock fracturing processes [2]. Different experimental and mathematical studies have been conducted to investigate the mechanism of crack growth under different levels of loading [3–5]. In 1995, the International Society for Rock Mechanics (ISRM) presented the Cracked Chevron Notched Brazilian Disc (CCNBD) test procedure to determine the mode I fracture toughness in rock [6]. In rock mechanics, fracture toughness is the fundamental parameter related to the materials resistance to fracture propagation

*Corresponding author
Email addresses: s.behraftar@uq.edu.au (Somayeh Behraftar), s.galindotorres@uq.edu.au (Sergio Galindo Torres), a.scheuermann@uq.edu.au (Alexander Scheuermann), d.williams@uq.edu.au (David J. Williams)

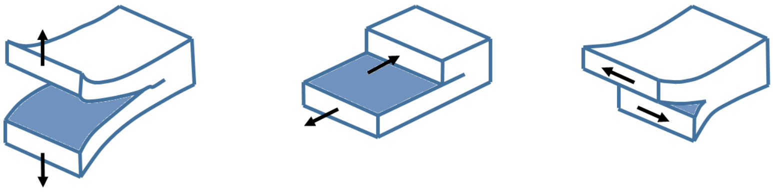

(a) (b) (c)

Fig. 1 Three main modes of crack propagation: (a) mode I (opening), (b) mode II (in-plane shearing), (c) mode III (tearing or anti-plane shearing)

from a pre-existing crack. The CCNBD test is used for determining mixed-mode fracture toughness by changing the inclination angle of the crack with respect to the direction of loading [3, 7, 8].

Since the fracture process is in principle discontinous, the Discrete Element Method (DEM) is considered to be an appropriate numerical approach to investigate the fracture processes in rocks. The use of continuous approaches such as the finite element or finite difference methods for studying the fracturing process in rocks may assist in assessing the weakening zone. However, cannot determine the fracture geometry during crack propagation, after fracture initiation. In fact, in continuum-based methods, the behaviour of discontinuous zones is not well described [9]. Among the discrete numerical techniques, the most effective and simple to apply to the crack propagation process in rock would be considering clusters of discrete particles in contact that are connected by cohesive or bonding forces. Even though cohesive forces have different physical origins, they all have the same effect, which is resisting the relative displacement that can occur between particles up to the time when they reach the threshold value [10]. In this paper, DSEM is used to model sphero-polyhedral-shaped particles extracted from Delaunay tessellations [11]. This is a departure from the traditional spherical element DEM approach and allows solid bodies without any internal voids. This DSEM technique has proven to be a very versatile discrete technique able to simulate non-convex shapes [12], fracture processes [10], and even the interaction between complex-shaped bodies and fluids [13].

In the present study, the DSEM approach is used to examine the macroscopic behaviour of specimens with pre-existing cracks subjected to static loading, with the crack opening displacement measured as a function of crack inclination. The measured crack opening displacement was successfully simulated using the DSEM. This is achieved by using dimensional analysis to derive relationships between the parameters and the responses and using those relationships to calibrate the DSEM. Also, the breakage of the specimens at the micro-scale is studied to investigate the fracture mode, and an open question is proposed on how to connect the micro-damage with the macroscopic modes used in continuous models.

In Section 2 of the paper, the experimental studies and results are reviewed. Section 3 includes an explanation of the simulation set-up and the numerical modelling of the CCNBD specimens using the DSEM method. This section includes some discussion and comparisons between both studies for mode I and II crack propagation. Section 4 presents the conclusions.

2. Experimental study

The CCNBD test was suggested in 1998 by the ISRM for measuring the fracture toughness of mode I (tensile) fractures [6]. A CCNBD specimen is a Brazilian disc with a notch cut using a circular saw from both sides in the middle of the specimen. By applying a compressive load across the circumference of the disc, a crack initiates and propagates from the notch towards the boundary of specimen. Fig. 2 illustrates the geometry of a CCNBD specimen. In the specimens considered for this study, the thickness of the notch is 1.5 mm. By changing the direction of loading relative to the crack inclination, different fracture modes can be obtained, including a mixed fracture mode [7, 14, 15].

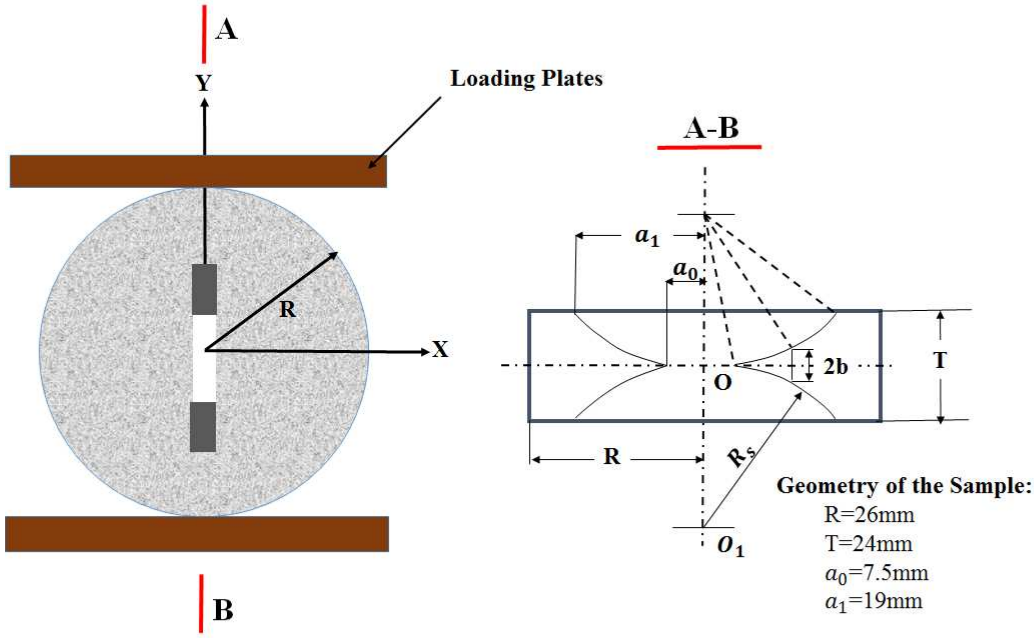

Fig. 2 CCNBD specimen geometry

In nature, pre-existing cracks in rock masses occur in arbitrary directions with respect to the loading direction. As a consequence, crack propagation is often in mixed mode rather than tensile mode. For the CCNBD specimens, the tangential stresses at the crack tip can be tensile or compressive depending on the crack inclination angle. These tangential stresses, in combination with shear stresses at the crack tip, cause a crack that propagates in a variety of mixed modes I-II failure trajectories [16]. Many studies have been carried out to find the fracture mode in rock masses with a pre-existing cracks or discontinuities [3–8, 17–23]. However, determining mixed-mode fracture characteristics of rock is still an open question. In the experimental studies reported in [24], CCNBD specimens were cut and then pure mode I, pure mode II and a range of mixed-mode loading conditions were investigated. In this study, the crack propagation trajectory under different conditions is simulated numerically and the failure paths in CCNBD specimens are traced. The numerical results are compared to the experimental results provided from reference [24].

2.1. *Experiments for determination of mixed-mode fracture of rocks*

In the experiments described in [24], CCNBD specimens were prepared from cores of Brisbane tuff and tested with various crack inclinations. The tests were carried out on different rock samples [24]. The geotechnical parameters of Brisbane tuff CCNBD specimens are presented in Table 1.

Table 1 Geotechnical parameters of Brisbane tuff CCNBD specimens tested [24].

	Youngs Modulus (GPa)	Poissons Ratio	UCS (MPa)*	BTS (MPa)**
Brisbane tuff	Max = 25	Max = 0.26	Max = 205	Max = 15
	Min = 19	Min = 0.22	Min = 97	Min = 8.0

* Uniaxial Compressive Strength.
** Brazilian Indirect Tensile Strength.

The experimental results presented in [24] included the fracture initiation and propagation in the Brisbane tuff CCNBD specimens tested under monotonic compressive loading, with the direction of loading relative to the crack inclination varied.

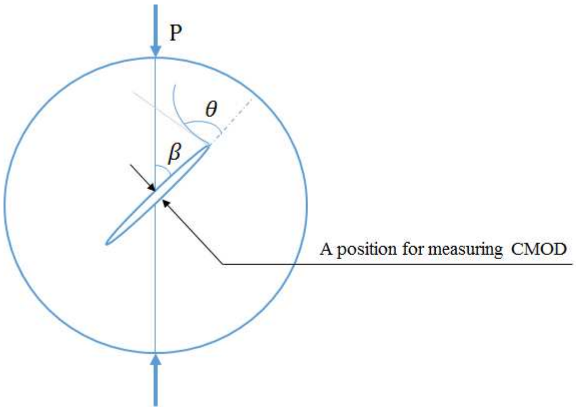

Fig. 3 Orientation of crack propagation in CCNBD specimens under diametral compression [24].

In these tests, the compressive load was applied continuously up until failure occurred. The inclination angles of the loading direction to the notch crack (β) tested were as 0°, 28°,30°, 33°, 45° and 70° [24]. During the experiments, the load and CMOD were recorded continuously. The compressive loads induced both tensile and shear stresses in the notch crack in the CCNBD specimens. According to previous studies, the crack initiates in Mode I and propagates in the direction parallel to the orientation of the compressive loading (Fig. 3) [23, 24].

Fig. 4 shows the measured load versus CMOD plots at different inclination angles(β) for Brisbane tuff CCNBD specimens [24]. As can be seen in Fig. 4 , depending on the inclination angle the crack can close or open further. When the crack is parallel to the loading direction, the fracture initiates at the ends of the notch, while when it is perpendicular the fracture initiation moves towards the middle of the notch. This feature needs to be reproduced by the proposed numerical model. Furthermore, opening occurred for $\beta \leq 30°$ while closing occurred for $\beta > 33°$, but for β between 30° and 33° both opening and closing displacements were observed. In these experiments, the maximum applied load was approximately $5KN$. It can be extracted from the results that crack propagation for $\beta > 33$ is in mode II (shearing mode) while crack propagation for $\beta < 30$ is in mode I (tensile mode) [24].

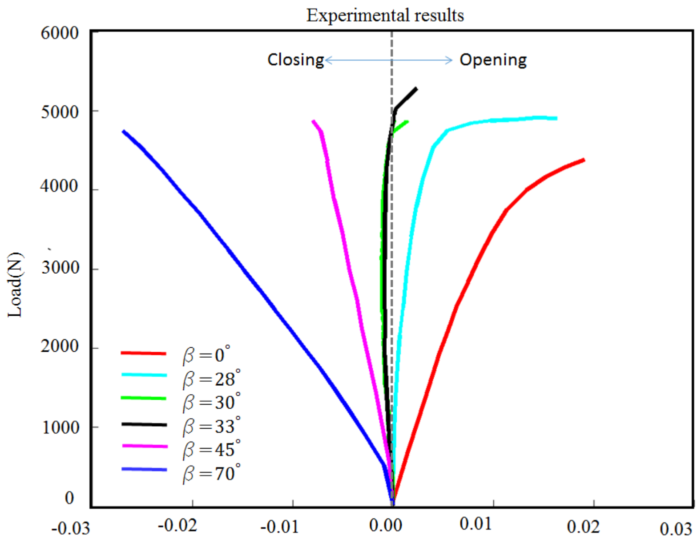

Fig. 4 Measured load versus CMOD at different inclination angles β for Brisbane tuff CCNBD specimens [24]

Fig. 4 illustrates that the peak failure load increases up to $\beta = 33°$ which, based on [24], suggests that failure at this inclination angle occurs mainly due to shearing.

3. Numerical simulation set up

The DSEM is used for the simulation. In three dimensions (3D), a sphero-polyhedra is a polyhedral-shaped particle formed by first eroding a cube, which is then dilated by sweeping the edges by a sphere, as shown in Fig. 5. By smoothing the edges of all of the geometric features with spheres, the definition of the contacts between the particles are simple and efficient.

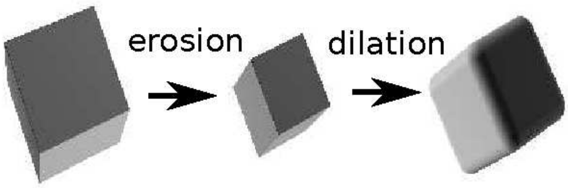

Fig. 5 A 3D sphero-cube formed by erosion to a distance equal to the radius of the sphere, followed by dilation with the same radius [12].

The collision and bonding forces existing between particles need to be defined to enable theiring investigation. The model assumes that there is an elastic force between two adjacent sphero-polyhedra that share a common face. This force is defined based on the Euler beam theory and is linearly dependent on the relative displacement (refer to [10] for more details). The tangential and normal strains are computed at the centroid of the common face at the beginning of the simulation. The coordinates of the centroids of all such faces are saved to memory. By moving or rotating the faces, the relative positions of the centroids will change, and the strains can be calculated from these relative displacements. The normal and tangential strains for each particle are summed to determine the total normal strain ε_n and the total tangential strain ε_t (Fig. 6), which are compared to the threshold value ε_{th} required for de-bonding, given by:

$$\left(\frac{\varepsilon_n}{\varepsilon_{th}}\right)^2 + \left(\frac{\varepsilon_t}{\varepsilon_{th}}\right)^2 > 1, \tag{1}$$

in which it is assumed that the failure surface is circular at the microscopic scale.

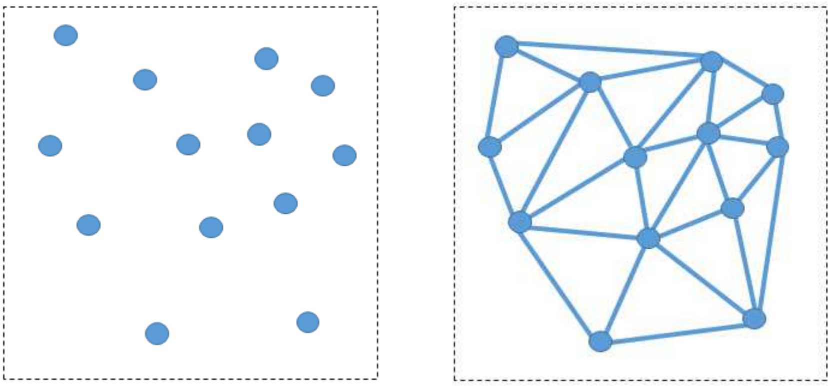

(a)

(b)

Fig. 7 Delaunay tessellation: (a) 10 random points, and (b) Delaunay tessellation.

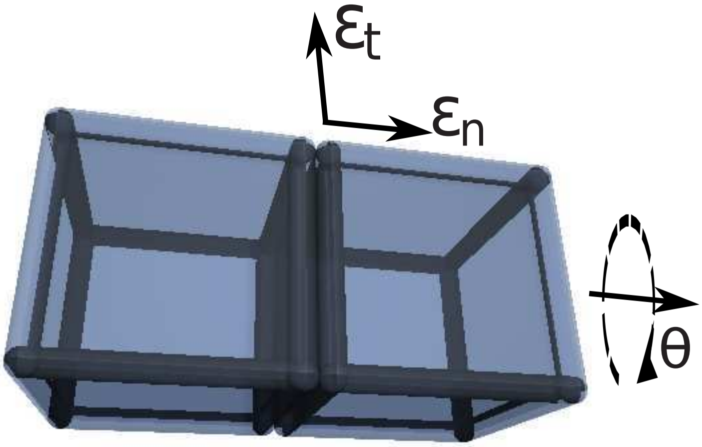

Fig. 6 Two sphero-cubes joined together by a flexible joint representing a bonding or cohesive interaction between them [10].

For modelling the specimen using the DSEM, an extruded two-dimensional (2D) Delaunay tessellation is used. A tessellation is a general term used to describe the division of space into a set of sub-spaces that do not overlap, but fill the space completely [25]. These tessellations can exist in two- and three-dimensional space. By applying the Delaunay tessellation, solid bodies with no internal voids can be modelled. In Fig. 8, the procedure for constructing Delaunay tessellations is demonstrated. Some points are distributed randomly in the space (Fig. 7(a)). The tessellation is obtained by connecting all pairs of closest points (Fig. 7(b)). The CCNBD specimen modelling is based on the specimen geometry given in Fig. 2. Fig. 8 shows the modelled specimen based on Delaunay-tessellation construction, which is made of a random array of 3,164 Delaunay sphero-polyhedra. Two plates at the top and bottom of the specimen apply the load to the specimen at a constant strain rate.

Simulations for different inclination angles (β) of the notch crack are conducted based on defined mirco-mechanical elasticity parameters [10]. The de-bonding condition (Equation 1) was used to define the initiation and further development of the crack. The results are visualised using VisIt [1] software (Fig. 9). For all inclination angles, it is observed

[1] https://wci.llnl.gov/simulation/computer-codes/visit

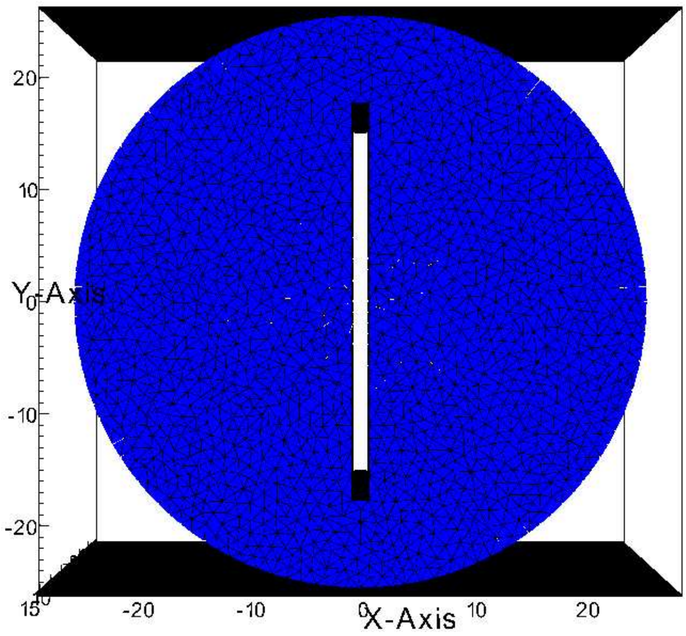

Fig. 8 Simulated CCNBD specimen using DSEM constructed by 3,164 Delaunay sphero-polyhedra.

that the crack propagates in a zig-zag pattern (Fig. 10), which does not represent the more smooth real propagation of a crack.

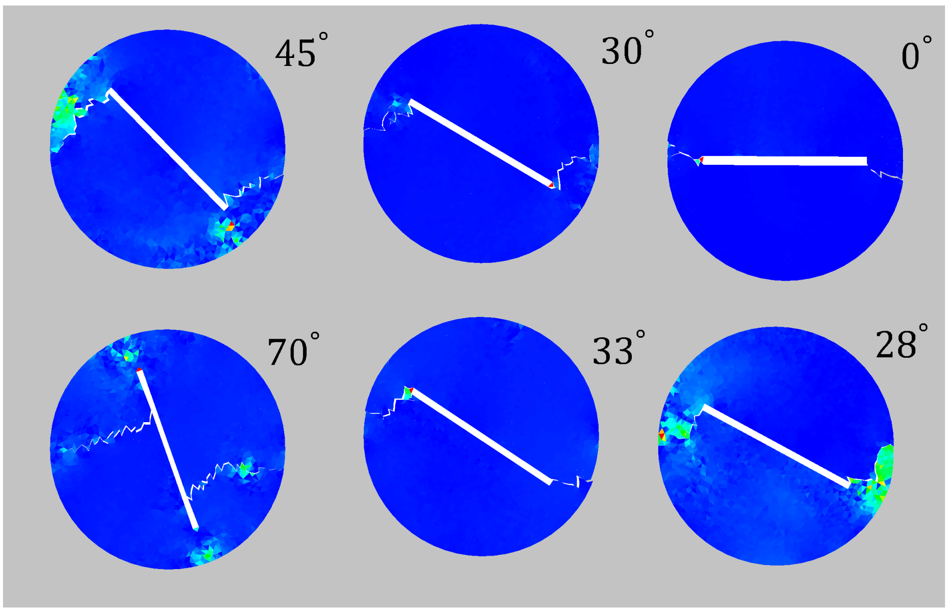

Fig. 9 Crack propagation for different inclination angles using de-bonding condition (Equation 1), visualised using VisIt software.

To address this simulated zig-zag crack propogation, the authors have modified the threshold expression given in Equation 2 to compare the normal and tangential strains (ε_n and ε_t, respectively) with the fixed threshold value ε_{th}. Equation 2 shows better agreement with the experimental observations (Fig. 10). However, although a better match is obtained, the physical reason for this improvement is still unknown and needs to be investigated further.

$$\text{De-bonding condition:} \quad \frac{|\varepsilon_n| + |\varepsilon_t|}{\varepsilon_{th}} > 1, \tag{2}$$

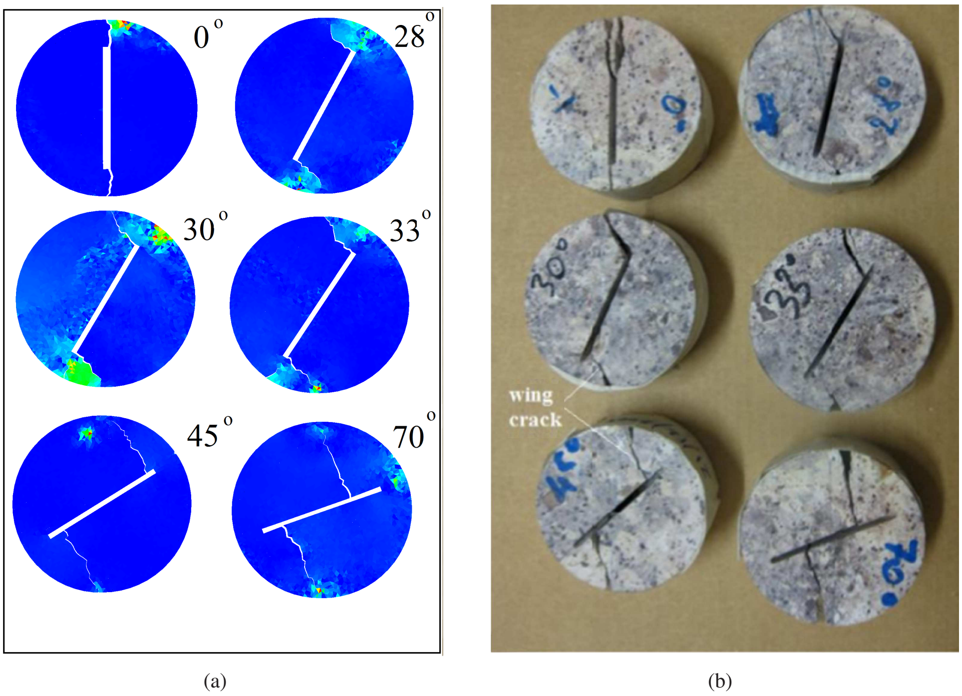

Fig. 10 Crack propagation for different inclination angles of loading: (a) results of simulations using de-bonding condition (Equation 2), and (b) experimental observations [24]

Fig. 10 illustrates that in both the experimental and simulated results, the crack initiates from the top of the pre-existing notch as long as $\beta \leq 33$, while for $\beta > 33$, the crack initiation point moves from the top to the centre of the notch. Although at the macro-scale the simulations could visually match the experimental observations, a quantitative comparison using the CMOD results failed. However, the analysis of the CMOD results is necessary to identify the fracture mode on the micro-scale. Obviously, there are several sets of micro-mechanical elasticity parameters that would allow a realistic representation of crack propagation. To enable quantitative comparisons between experiment and simulation, the DSEM model needs to be calibrated based on the crack opening process during the loading phase quantified by the CMOD value.

3.1. Micro-macro relationship and DSEM calibration

In using the DSEM some micro-mechanical parameters must be specified to match macroscopic parameters such as Youngs modulus (E), Poissons ratio (υ), compressive strength (σ_c), tensile strength (σ_t) and the failure envelope. The micro-mechanical parameters describing the interaction between two sphero-polyhedral particles are the normal and tangential stiffnesses (K_n, K_t) to define the forces that detect collision, the normal and tangential elastic moduli (B_n, B_t) used to define the normal and tangential bonding forces between particles, and the Coulomb friction coefficient (μ). These micro-mechanical parameters influence the overall failure envelope [10]. For a realistic representation of the material behaviour it is absolutely essential to calibrate these parameters. This was done using dimensional analysis based on the Buckingham Π theorem [26]. The concept of this theorem is that the number of dimensionless parameters is the dimension of the nullspace of the dimensional matrix. Dimensionless parameters defined with the above micro-mechanical parameters are used to compare the results of virtual experiments with those of real experiments.

The CMOD is used to calibrate the micro-mechanical model. Since the friction coefficient (μ) has the dominant effect on the post-failure behaviour of the specimen, it can be removed from this analysis. Furthermore, based on previous studies K_t does not affect the elastic behaviour of the material [10], and it, also, is not considered in the analysis.

The CMOD also depends on other parameters related to the geometry of the specimen (radius of the sample, R and the load, F). After finding the null space of the dimensional matrix, the proposed approach is based on four independent parameters $\{\frac{B_t}{B_n}, \frac{K_n}{B_n R}, \frac{B_n F}{K_n^2}, \frac{CMOD}{R}\}$. Since, the CMOD was measured under static loading before failure, $\frac{B_n F}{K_n^2}$ can be removed from the calculations. Therefore, the following dimensionless functional relationship linking the microscopic parameters to the macroscopic behaviour of the material can be postulated for the DSEM:

$$\frac{CMOD}{R} = \Phi_{CMOD}\left(\frac{B_t}{B_n}, \frac{K_n}{B_n R}\right) \tag{3}$$

where Φ_{CMOD} is a dimensionless function. The specific form of the dimensionless relationship in Equation 3 is obtained from the results of numerical simulations of the CCNBD test. As can be seen in Equation 3, it is sufficient to change B_t and K_n to obtain the variation of CMOD for a specified load level. The approach adopted in this study consists of two steps: (i) the virtual experiment must represent realistic material behaviour in terms of crack development, and (ii) the CMOD must match the experimental results. To achieve this, different micro-mechanical elasticity parameters (K_n/K_n^r and B_t/B_t^r) are chosen to simulate the CCNBD test for a notch crack inclined at 70°, as shown in Fig. 11 (K_n^r and B_t^r are initial values (Table 2) that are chosen based on results published in [10]).

Table 2 Initial values of parameters used in simulations [10].

Parameter	Value	Unit
${K_n}^r$	1.0×10^7	N/m
${K_t}^r$	1.0×10^7	N/m
e^r	0.2	
μ^r	0.3	
${B_n}^r$	50.0	GPa
${B_t}^r$	100.0	GPa
Δt^r	0.5×10^{-11}	s
${\varepsilon_{th}}^r$	0.015	

Fig. 11 illustrates that for a wide range of the two micro-mechanical elasticity parameters, the simulated fracture geometry matches the experimental observations. However, in some cases the fracture geometry is different from the experimental observations (wrong fracture geometry as seen in Fig. 12) and in some cases no breakage occurs, although this can easily be adjusted by changing the ε_{th} parameter defining the de-bonding condition (Equation 2). Based on this result, it can be concluded that the fracture geometry, as a macroscopic manifestation of material failure, is affected more by the de-bonding condition than by the micro-mechanical elasticity parameters. This cannot be said of the deformation represented by the CMOD, which is highly sensitive to the microscopic parameters, as will be shown later.

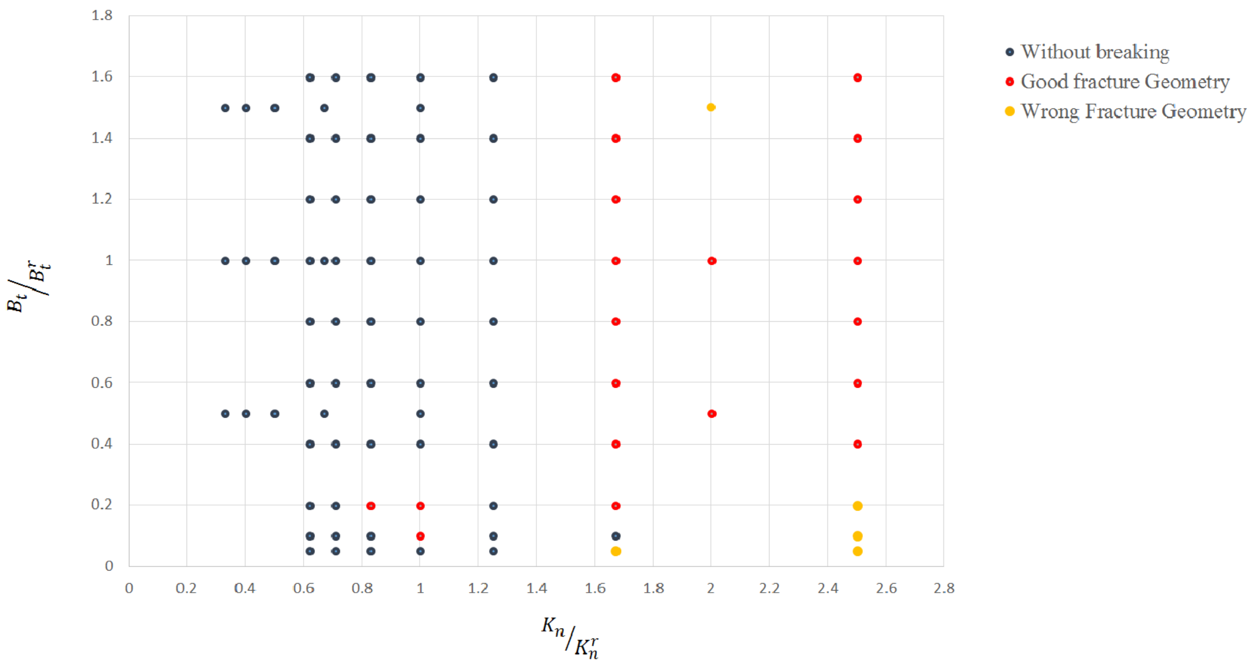

Fig. 11 Fracture geometry for different micro-mechanical elasticity parameters.

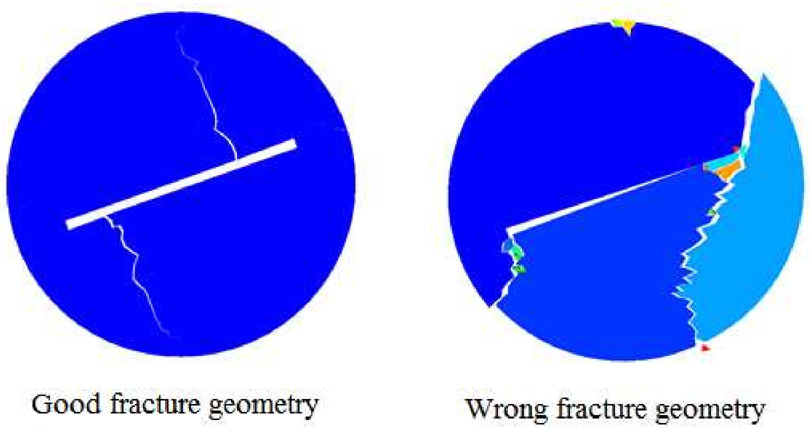

Fig. 12 Difference between fracture geometry that matches experimental observations, and wrong fracture geometry for $\beta = 70°$.

The next step is to calibrate the CMOD for a specific load. This load was chosen to be 2000 N, which is reached well before failure as observed in the experiments ([24] and Fig. 4). The CMOD for different B_t and K_n at two different inclination angles ($\beta = 0°, \beta = 70°$) are calculated (Fig. 13(a) and 13(b)). It is interesting to observe that for both inclination angles $\beta = 0°, \beta = 70°$ the CMOD is affected by K_n. However, for different B_t the CMOD is constant apart from for small values of B_t. Therefore, it can be said that the CMOD is most sensitive to the contact stiffness in the normal direction (K_n).

In order to select the right combination of B_t and K_n, the experimental results (Fig. 13(a) and 13(b)) for both inclination angles ($\beta = 0°, \beta = 70°$) are selected for simulation. Table 3 shows the experimental CMOD values for the selected B_t and K_n values.

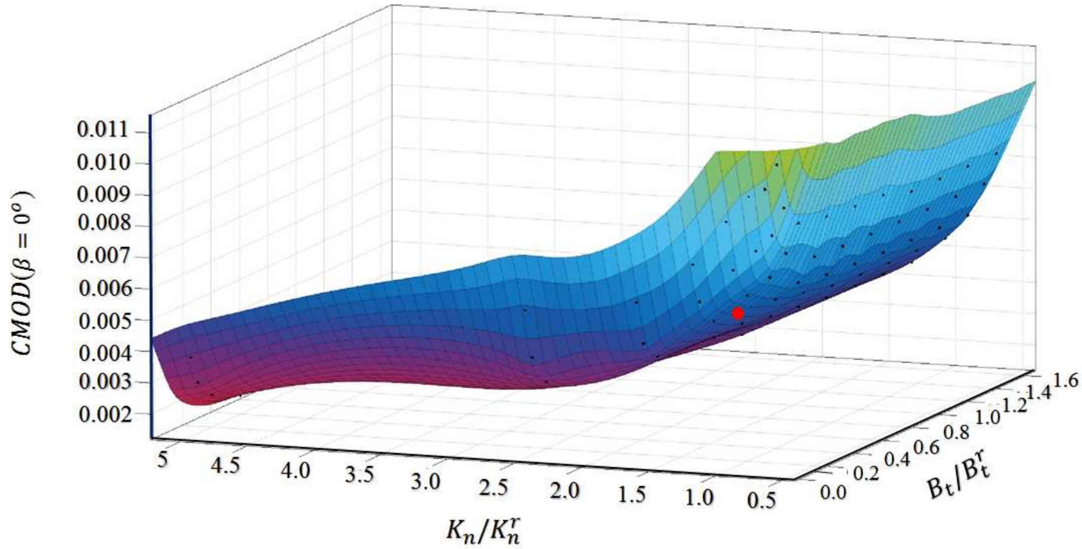

(a)

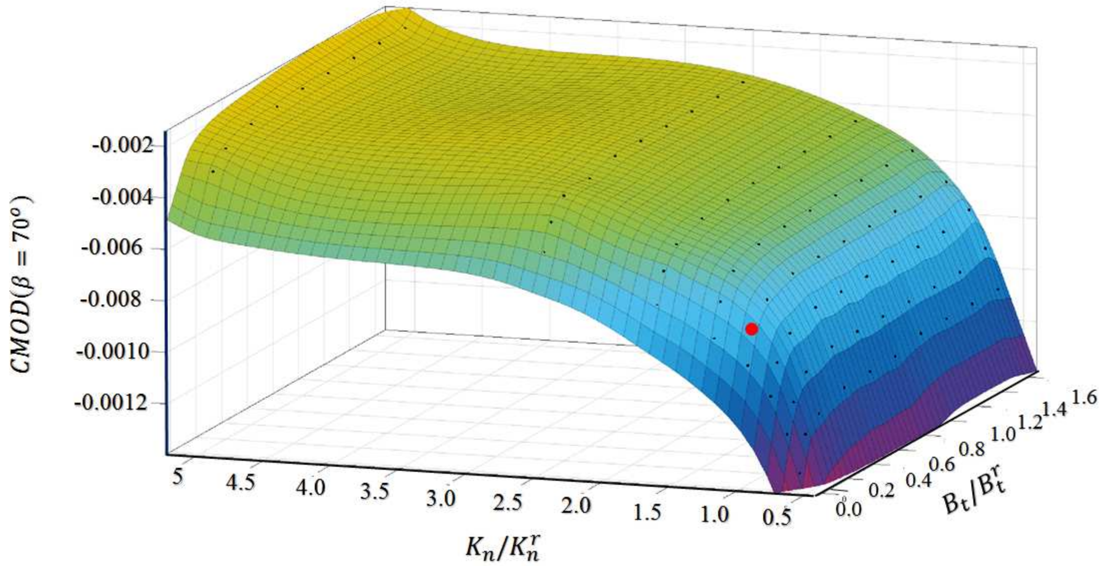

(b)

Fig. 13 CMOD as a function of microscopic parameters for: (a) $\beta = 0°$, and (b) $\beta = 70°$ (red dot points show desired matching data for calibration).

Table 3 CMOD values from laboratory tests

Load (N)	Angle (°)	CMOD (*mm*)
2000	$\beta = 0$	0.005
2000	$\beta = 70$	-0.009^{*}

* negative sign depicts the cracks are closing during the loading process.

According to Fig. 13 and Table 3, it can be seen that the simulated CMOD are equal to the experimental values at $K_n/K_n^r = 1.0$ and $B_t/B_t^r = 0.1$. Considering that Fig. 11 uses the selected parameters, good fracture geometry is also simulated.

Table 4 Set of parameters used in the simulations (refer to [10] for more detailed information).

Parameter	Value	Unit
K_n	1.00×10^{7}	N/m
K_t	1.00×10^{7}	N/m
e	0.20	
μ	0.3	
B_n	50.0	GPa
B_t	10.0	GPa
Δt	0.5×10^{-11}	s
ε_{th}	0.015	

3.2. *Validity of dimensional analysis*

To check the validity of the introduced dimensionless numbers based on the microscopic parameters, the CMOD is calculated for $\beta = 0°$ using the values summarised in Table 4 and another set of parameters the double all dimensionless terms. As can be seen in Fig. 14, the calculated CMOD values for both data sets do not differ significantly while the experimental values are reasonably well matched. This result shows that the use of dimensionless numbers for simplifying processes at the micro-scale is justified and the relationship defined in Equation 3 is adequate and correct for the simulation of the CCNBD test on Brisbane tuff.

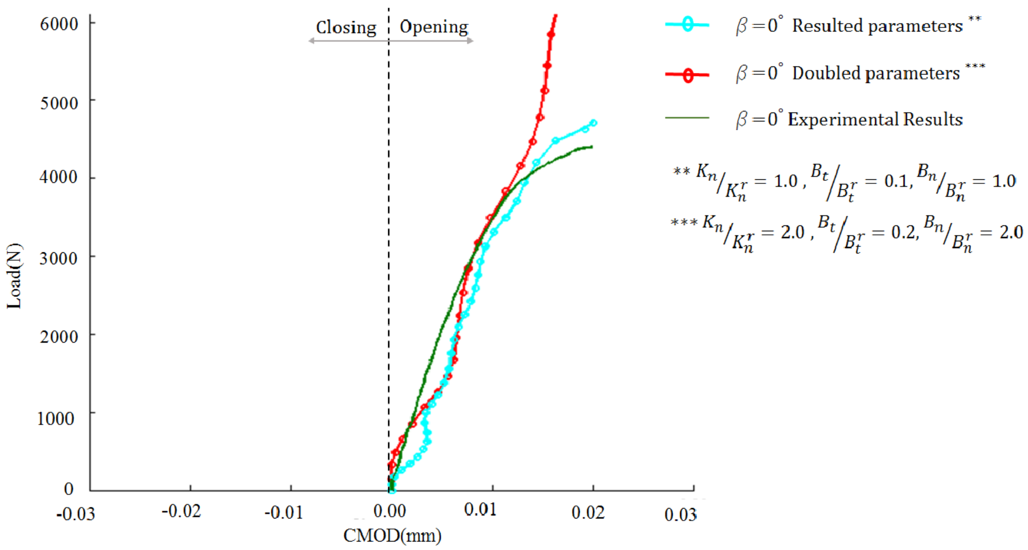

Fig. 14 CMOD versus load for different parameter sets

The parameters presented in Table 4 are used as inputs for the simulation to study the CMOD for different inclination angles of the notch cracks relative to the load. As can be seen in Fig. 4 and Fig. 15, the calculated and measured CMOD values match reasonably well. Based on these results, it can be said that the relationship between micro- and meso-scale parameters of the material are well understood for the CCNBD testing of Brisbane tuff.

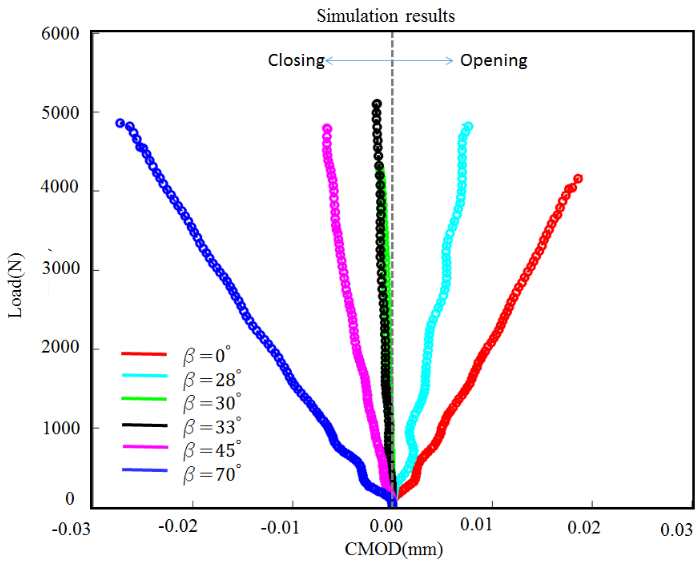

Fig. 15 Simulated load versus CMOD at different inclination angles β for Brisbane tuff CCNBD specimens

Following this important calibration and validation step, some microscopic aspects characterising the fracture propagation can be extracted from the simulation results. When the loading on the CCNBD specimen increases, tangential and normal forces between particles at the micro-scale increase, which causes normal and tangential strain in the particles. Therefore, when these strains exceed the threshold value ε_{th} either in the normal or tangential direction, breakage occurs. To determine under which mode the fracture occurs at the micro-scale, it is sufficient to observe which strain is higher for the set of all shared faces.

4. Conclusion

In this paper Cracked Chevron Notched Brazilian Discs (CCNBD) were modelled using the Discrete Sphero-polyhedral Element Method (DSEM). In the proposed model, a collection of particles was generated from an extruded Delaunay tessellation, which allows the modelling of rock specimens that do not have internal porosity.

The breaking process of the CCNBD specimen was tracked using the DSEM. Simulation of the CCNBD tests on Brisbane tuff showed that the proposed method was capable of reproducing the results obtained from the experimental tests. Crack propagation trajectory during loading was simulated and showed good agreement with the experimental results. Using the DSEM, the macroscopic behaviour of the material; namely, the trajectory of the crack propagation during loading based on parameters of the material, can be predicted for natural pre-existing cracks in different directions.

The Crack Mouth Opening Displacement (CMOD) is the meso-scale feature recorded during CCNBD tests to monitor the deformation of the sample. The simulation model was calibrated using this feature, based on a dimensional analysis of microscopic parameters. The simulated CMOD values show good agreement with the experiments for different inclination angles between the direction of loading and the orientation of the notch cracks. It is important to mention that the CMOD is very sensitive to the microscopic parameters, while the fracture geometry is not.

Acknowledgements

This work was funded by Australian Research Council (ARC) Discovery Project DP140100490 Qualitative and quantitative modelling of hydraulic fracturing of brittle materials. The software used for all the simulations presented in this paper is based on the open source library MechSys (http://mechsys.nongnu.org/index.shtml) developed by the authors. The simulations were carried out on the Macondo high performance computing cluster within the School of Civil Engineering at The University of Queensland. E.A.G. Marques acknowledges the support from the Brazilian CAPES Agency. The first author thanks Dr Nazife Erarslan for providing the experimental data.

5. References

[1] BN Whittaker, RN Singh, and G Sun. Rock fracture mechanics-principles, design and applications. 1992.

[2] EZ Lajtai. A theoretical and experimental evaluation of the griffith theory of brittle fracture. *Tectonophysics*, 11(2):129–156, 1971.

[3] MR Ayatollahi and MRM Aliha. Fracture toughness study for a brittle rock subjected to mixed mode i/ii loading. *International Journal of Rock Mechanics and Mining Sciences*, 44(4):617–624, 2007.

[4] IL Lim, IW Johnston, SK Choi, and JN Boland. Fracture testing of a soft rock with semi-circular specimens under three-point bending. part 2mixed-mode. In *International journal of rock mechanics and mining sciences & geomechanics abstracts*, volume 31, pages 199–212. Elsevier, 1994.

[5] HN Atahan, MA Tasdemir, C Tasdemir, N Ozyurt, and S Akyuz. Mode i and mixed mode fracture studies in brittle materials using the brazilian disc specimen. *Materials and structures*, 38(3):305–312, 2005.

[6] Qi-Zhi Wang. Stress intensity factors of the isrm suggested ccnbd specimen used for mode-i fracture toughness determination. *International Journal of Rock Mechanics and Mining Sciences*, 35(7):977–982, 1998.

[7] Soo-Ho Chang, Chung-In Lee, and Seokwon Jeon. Measurement of rock fracture toughness under modes i and ii and mixed-mode conditions by using disc-type specimens. *Engineering geology*, 66(1):79–97, 2002.

[8] K Khan and NA Al-Shayea. Effect of specimen geometry and testing method on mixed mode i–ii fracture toughness of a limestone rock from saudi arabia. *Rock mechanics and rock engineering*, 33(3):179–206, 2000.

[9] F Camborde, C Mariotti, and FV Donzé. Numerical study of rock and concrete behaviour by discrete element modelling. *Computers and geotechnics*, 27(4):225–247, 2000.

[10] SA Galindo-Torres, DM Pedroso, DJ Williams, and L Li. Breaking processes in three-dimensional bonded granular materials with general shapes. *Computer Physics Communications*, 183(2):266–277, 2012.

[11] SA Galindo-Torres and DM Pedroso. Molecular dynamics simulations of complex-shaped particles using voronoi-based spheropolyhedra. *Physical Review E*, 81(6):061303, 2010.

[12] SA Galindo-Torres, F Alonso-Marroquín, YC Wang, D Pedroso, and JD Munoz Castano. Molecular dynamics simulation of complex particles in three dimensions and the study of friction due to nonconvexity. *Physical Review E*, 79(6):060301, 2009.

[13] SA Galindo-Torres. A coupled discrete element lattice boltzmann method for the simulation of fluid–solid interaction with particles of general shapes. *Computer Methods in Applied Mechanics and Engineering*, 265:107–119, 2013.

[14] RJ Fowell and C Xu. The cracked chevron notched brazilian disc test-geometrical considerations for practical rock fracture toughness measurement. In *International journal of rock mechanics and mining sciences & geomechanics abstracts*, volume 30, pages 821–824. Elsevier, 1993.

[15] MR Ayatollahi and MRM Aliha. On the use of brazilian disc specimen for calculating mixed mode i–ii fracture toughness of rock materials. *Engineering Fracture Mechanics*, 75(16):4631–4641, 2008.

[16] Naser A Al-Shayea. Crack propagation trajectories for rocks under mixed mode i–ii fracture. *Engineering Geology*, 81(1):84–97, 2005.

[17] R Hasanpour and N Choupani. Mixed-mode study of rock fracture mechanics by using the modified arcan specimen test. *World Acad Sci Eng Tech*, 41:764–769, 2008.

[18] Tobias Backers. *Fracture toughness determination and micromechanics of rock under mode I and mode II loading*. PhD thesis, Universitätsbibliothek, 2005.

[19] ML Benzeggagh and M Kenane. Measurement of mixed-mode delamination fracture toughness of unidirectional glass/epoxy composites with mixed-mode bending apparatus. *Composites Science and Technology*, 56(4):439–449, 1996.

[20] S Suresh, CF Shih, A Morrone, and NP O'Dowd. Mixed-mode fracture toughness of ceramic materials. *Journal of the American Ceramic Society*, 73(5):1257–1267, 1990.

[21] N Erarslan and DJ Williams. Mechanism of rock fatigue damage in terms of fracturing modes. *International Journal of Fatigue*, 43:76–89, 2012.

[22] Rohola Hasanpour and Naghdali Choupani. Rock fracture characterization using the modified arcan test specimen. *International Journal of Rock Mechanics and Mining Sciences*, 46(2):346–354, 2009.

[23] Qiuhua Rao, Zongqi Sun, O Stephansson, Chunlin Li, and B Stillborg. Shear fracture (mode ii) of brittle rock. *International Journal of Rock Mechanics and Mining Sciences*, 40(3):355–375, 2003.

[24] Nazife Erarslan. *Static and cyclic laboratory testing of Brisbane rocks*. PhD thesis, Civil Engineering, University of Queensland, 2011.

[25] Catherine O'Sullivan. *Particulate discrete element modelling*. Taylor & Francis, 2011.

[26] Edgar Buckingham. On physically similar systems; illustrations of the use of dimensional equations. *Physical Review*, 4(4):345–376, 1914.